A&A, 684, L18 (2024)
https://doi.org/10.1051/0004-6361/202449350

Astronomy & Astrophysics

LETTER TO THE EDITOR

Spectroscopic observations of progenitor activity 100 days before a Type Ibn supernova⋆

S. J. Brennan[1], J. Sollerman[1], I. Irani[2], S. Schulze[3,4], P. Chen[2], K. K. Das[5], K. De[6], C. Fransson[1], A. Gal-Yam[2], A. Gkini[1], K. R. Hinds[7], R. Lunnan[1], D. Perley[7], Y. J. Qin[5], R. Stein[5], J. Wise[7], L. Yan[8], E. A. Zimmerman[2], S. Anand[5], R. J. Bruch[2], R. Dekany[8], A. J. Drake[5], C. Fremling[8], B. Healy[9], V. Karambelkar[5], M. M. Kasliwal[5], M. Kong[5], S. R. Kulkarni[5], F. J. Masci[10], R. S. Post[11], J. Purdum[8], R. Michael Rich[12], and A. Wold[10]

[1] The Oskar Klein Centre, Department of Astronomy, Stockholm University, AlbaNova 106 91, Stockholm, Sweden
e-mail: sean.brennan@astro.su.se
[2] Department of Particle Physics and Astrophysics, Weizmann Institute of Science, 234 Herzl St, 7610001 Rehovot, Israel
[3] Center for Interdisciplinary Exploration and Research in Astrophysics (CIERA), Northwestern University, 1800 Sherman Ave., Evanston, IL 60201, USA
[4] The Oskar Klein Centre, Department of Physics, Stockholm University, Albanova University Center, 106 91 Stockholm, Sweden
[5] Division of Physics, Mathematics and Astronomy, California Institute of Technology, Pasadena, CA 91125, USA
[6] MIT-Kavli Institute for Astrophysics and Space Research, 77 Massachusetts Ave., Cambridge, MA 02139, USA
[7] Astrophysics Research Institute, Liverpool John Moores University, IC2, Liverpool Science Park, 146 Brownlow Hill, Liverpool L3 5RF, UK
[8] Caltech Optical Observatories, California Institute of Technology, Pasadena, CA 91125, USA
[9] School of Physics and Astronomy, University of Minnesota, Minneapolis, MN 55455, USA
[10] IPAC, California Institute of Technology, 1200 E. California Blvd, Pasadena, CA 91125, USA
[11] Post Observatory, Lexington, MA 02421, USA
[12] Department of Physics & Astronomy, University of California Los Angeles, PAB 430 Portola Plaza, Los Angeles, CA 90095-1547, USA

Received 26 January 2024 / Accepted 23 March 2024

ABSTRACT

Obtaining spectroscopic observations of the progenitors of core-collapse supernovae is often unfeasible, due to an inherent lack of knowledge as to what stars experience supernovae and when they will explode. In this Letter we present photometric and spectroscopic observations of the progenitor activity of SN 2023fyq before the He-rich progenitor explodes as a Type Ibn supernova. The progenitor of SN 2023fyq shows an exponential rise in flux prior to core collapse. Complex He I emission line features are observed in the progenitor spectra, with a P Cygni-like profile, as well as an evolving broad base with velocities of the order of 10 000 km s^{-1}. The luminosity and evolution of SN 2023fyq is consistent with a Type Ibn, reaching a peak r-band magnitude of −18.8 mag, although there is some uncertainty regarding the distance to the host, NGC 4388, which is located in the Virgo cluster. We present additional evidence of asymmetric He-rich material being present both prior to and after the explosion of SN 2023fyq, which suggests that this material survived the ejecta interaction. Broad [O I], C I, and the Ca II triplet lines are observed at late phases, confirming that SN 2023fyq was a genuine supernova, rather than a non-terminal interacting transient. SN 2023fyq provides insight into the final moments of a massive star's life, demonstrating that the progenitor is likely highly unstable before core collapse.

Key words. circumstellar matter – supernovae: general – supernovae: individual: ZTF22abzzvln

1. Introduction

Massive stars (≳8–10 $M_\odot$) will eventually end their lives as core-collapse supernovae (CCSNe; Woosley & Weaver 1995; Heger et al. 2003; Janka 2012; Crowther 2012). With the increasing capabilities of photometric transient surveys (Bellm 2014; Chambers et al. 2016; Tonry et al. 2018), a growing sample of supernova (SN) progenitors have been observed experiencing outbursts in the weeks and years prior to their ultimate core collapse (Foley et al. 2007; Pastorello et al. 2007; Mattila et al. 2008; Ofek et al. 2013, 2014; Fraser et al. 2013; Margutti et al. 2014; Strotjohann et al. 2021; Fransson et al. 2022; Jacobson-Galán et al. 2022; Smith et al. 2022; Hiramatsu et al. 2023). These precursor events are difficult to explain, and are a relatively new area of stellar astrophysics (Dessart et al. 2010; Quataert & Shiode 2012; Leung et al. 2021; Strotjohann et al. 2021; Tsang et al. 2022). They are, however, often invoked to explain the presence of complex circumstellar material (CSM) shortly before collapse (Matsumoto & Metzger 2022; Hiramatsu et al. 2023). Precursor activity is likely accompanied by violent mass ejections via a currently unclear mechanism. Potential scenarios include binary interaction (Yoon et al. 2010, 2017; Smith 2011; Kashi et al. 2013; Zapartas et al. 2021; Tsuna et al. 2024), outbursts from luminous blue variables

⋆ The spectroscopic and photometric data underlying this article are available in the Weizmann Interactive Supernova Data Repository (WISeREP: https://www.wiserep.org/object/23708; Yaron & Gal-Yam 2012).

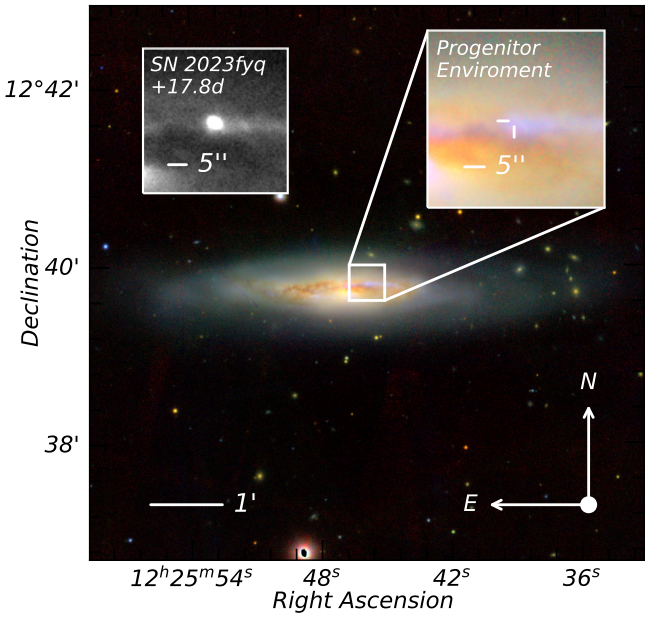

Fig. 1. Composite *giy* color image of the host galaxy of SN 2023fyq from the Pan-STARRS survey, with the transient environment given in the top-right inset. An *r*-band image of SN 2023fyq from the NOT/ALFOSC from 16 August 2023 is given in the top-left inset.

(Humphreys & Davidson 1994; Smith et al. 2010, 2022; Kilpatrick et al. 2018), and instabilities towards the end of a massive star's life (Woosley et al. 2007; Smith & Arnett 2014; Müller et al. 2016; Fuller & Ro 2018; Leung et al. 2021; Wu & Fuller 2022).

This Letter presents spectral (photometric) observations of the progenitor of a Type Ibn SN several months (years) before core collapse, as well as observations of SN 2023fyq itself. The precursor activity of SN 2023fyq[1] was discovered with the Zwicky Transient Facility (ZTF; Graham et al. 2019; Bellm et al. 2019; Masci et al. 2019; Dekany et al. 2020) at RA = 12:25:45.874, Dec = +12:39:48.87 (J2000) on 17 April 2023, at g = 19.51 mag (AB; De 2023). Spectroscopic observations of the progenitor were obtained as part of the Census of the Local Universe (CLU) survey (De et al. 2020) as it satisfied the selection criteria: a low-luminosity transient in a nearby galaxy. SN 2023fyq was later classified by the Nordic optical telescope Unbiased Transient Survey 2 (NUTS2) as a Type Ib-pec SN (Valerin et al. 2023) on 25 July 2023, around 5 days pre-peak. SN 2023fyq occurred approximately 10″ from the core of the active spiral galaxy NGC 4388 (Damas-Segovia et al. 2016) in the Virgo Cluster, as presented in Fig. 1. For consistency with the literature, we assumed a distance of 17.2 Mpc to NGC 4388 (Lianou et al. 2019; Böhringer et al. 1997) and a distance modulus (μ) of 31.2 mag, which gives SN 2023fyq a peak r-band magnitude of −18.8 mag. However, this distance is uncertain and may be as high as 25 Mpc (e.g. Ekholm et al. 2000), meaning SN 2023fyq may be ∼1.5 mag more luminous. We corrected for foreground Milky Way (MW) extinction using R_V = 3.1, $E(B-V)_{\rm MW}$ = 0.029 mag (Schlafly & Finkbeiner 2011) with the extinction law given by Cardelli et al. (1989). Measurements of host emission lines indicate a substantial host attenuation, as inferred from the Balmer (Hα/Hβ) decrement, of $E(B-V)_{\rm host} \approx 0.4 \pm 0.1$ mag (Osterbrock 1989). We corrected for this extinction in a similar fashion as the MW extinction, using an R_V = 2. We adopted a redshift of z = 0.0084, and the rest-frame phase is reported with respect to the r-band peak magnitude on 30 July 2023 ($t_{\rm peak}$ = 60155.1).

[1] Also known as ZTF22abzzvln, ATLAS23rwh, and PS23fnw.

2. Observations

2.1. Photometric observations

Science-ready images taken as part of the ZTF survey were obtained in *gri* from the NASA/IPAC Infrared Science Archive[2] service. Template-subtracted photometry was performed using the AutoPhOT pipeline (Brennan & Fraser 2022). Photometry from the ATLAS forced-photometry server[3] (Tonry et al. 2018; Smith et al. 2020; Shingles et al. 2021) was obtained in the *c* and *o* bands. Several epochs of optical photometry were obtained, with (i) the Alhambra Faint Object Spectrograph and Camera (ALFOSC) on the 2.56 m Nordic Optical Telescope (NOT) in *gri*, (ii) the Liverpool Telescope (LT) with the optical imaging component of the Infrared-Optical imager: Optical (IO:O) in *griz*, and (iii) the Spectral Energy Distribution Machine (SEDM; Blagorodnova et al. 2018; Rigault et al. 2019) on the Palomar 60-inch (P60) telescope in *gri*. We also obtained *gri* images from a 32-inch Ritchey-Chretien telescope (RC32) at Post Observatory in Mayhill, New Mexico. UV photometry was acquired using the Ultra-violet Optical Telescope (UVOT) on board the *Neil Gehrels Swift* Observatory (Gehrels et al. 2004; Roming et al. 2005). We reduced the images using the *Swift* HEAsoft[4] V. 6.26.1. tool set, as detailed in Irani et al. (2023). A UV template image was constructed using archival observations prior to MJD 59100 and after the SN declined to the host level. We then removed the local host-galaxy contribution by subtracting the SN site flux from the fluxes of the individual epochs.

2.2. Spectroscopic observations

Follow-up spectra were obtained using NOT/ALFOSC, the Low Resolution Imaging Spectrometer (LRIS; Oke et al. 1995) on the 10 m Keck telescope, the Double Spectrograph (DBSP) on the Palomar 200-inch telescope (P200), the Kast spectrograph at Lick Observatory, the Gemini Multi-Object Spectrographs (GMOS) mounted on the Gemini North 8 m telescope (Hook et al. 2004), and P60/SEDM (Blagorodnova et al. 2018). Spectra were reduced in a standard manner using LPipe (Perley 2019), DBSP_DRP (Mandigo-Stoba et al. 2022), and PypeIt (Prochaska et al. 2020a,b) for Keck/LRIS, P200/DBSP, and NOT/ALFOSC spectra; pysedm (Rigault et al. 2019; Kim et al. 2022) for SEDM spectra; the UCSC spectral pipeline (Siebert et al. 2019) for the Kast/Lick spectrum; and DRAGONS (Labrie et al. 2019) for our GEMINI/GMOS spectrum. Observations using the P60, P200, and Keck telescopes were coordinated using the FRITZ data platform (van der Walt et al. 2019; Coughlin et al. 2023).

NGC 4388 was observed with the Multi Unit Spectroscopic Explorer (MUSE) at the 8.2 m ESO Very Large Telescope (VLT) on 12 March 2022 (ID. 108.229J, PI. Venturi). Observations were reduced using MUSE pipeline v2.8.7 and the ESO workflow engine ESOReflex (Freudling et al. 2013; Weilbacher et al. 2020). We extracted all spectra with MUSE Python Data Analysis Framework (MPDAF) version 3.6 (Bacon et al. 2016). The spectrum of the SN site was extracted with a circular aperture. The aperture radius of 0.5″ translates to a physical scale of

[2] https://irsa.ipac.caltech.edu/applications/ztf/
[3] https://fallingstar-data.com/forcedphot/
[4] https://heasarc.gsfc.nasa.gov/docs/software/heasoft/

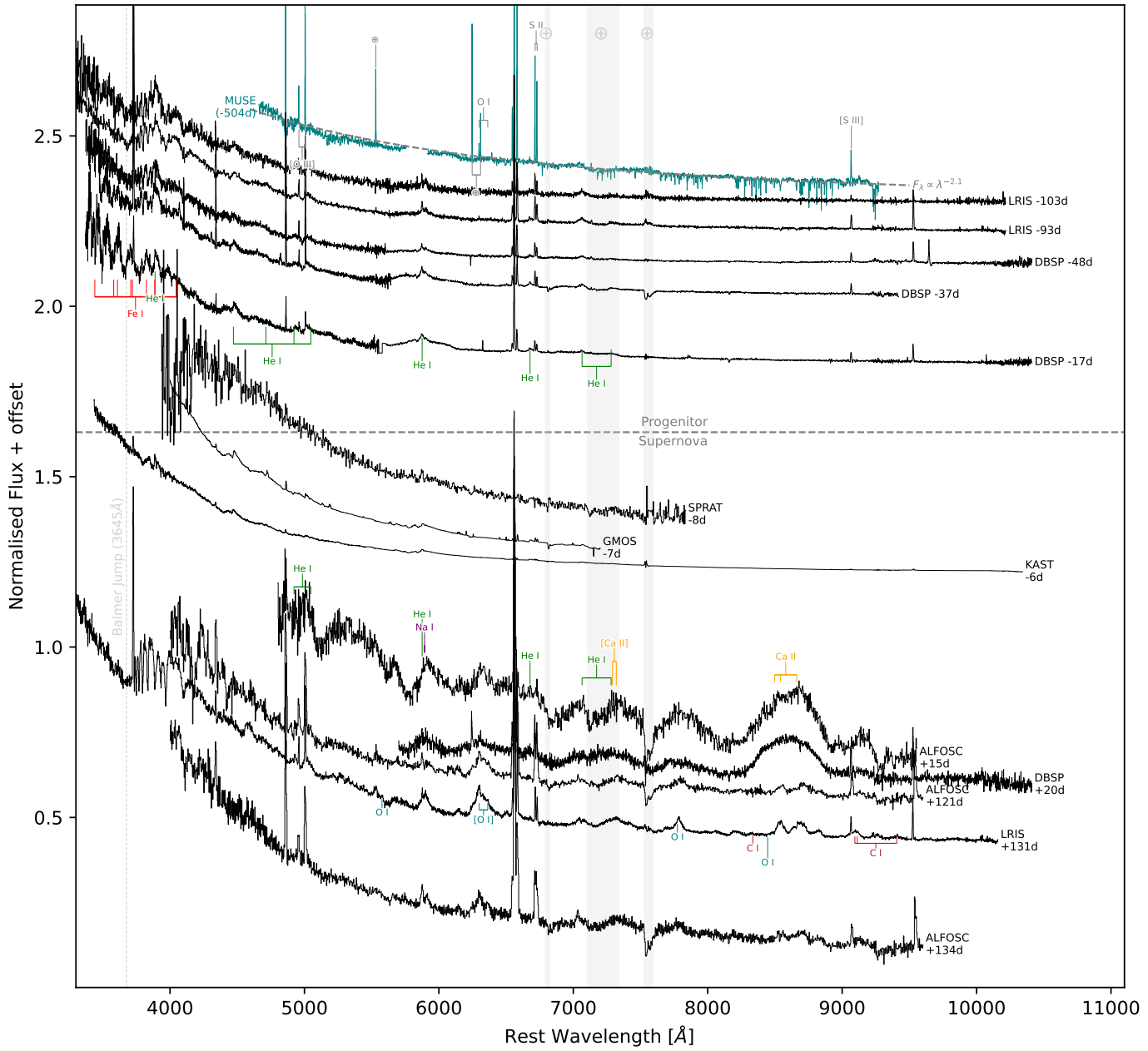

Fig. 2. Spectral observations of SN 2023fyq and its progenitor. Each spectrum has been normalised and offset for clarity, as well as corrected for redshift and extinction. We mark regions of telluric contamination using the ⊕ symbol and grey vertical bands.

89.5 pc at the projected distance of SN 2023fyq, which is comparable to the largest giant molecular clouds in the MW. Spectroscopic observations for the progenitor activity and SN 2023fyq are presented in Fig. 2.

3. Results and discussion

3.1. The photometric evolution of SN 2023fyq and its progenitor activity

Figure 3 shows the photometric evolution of SN 2023fyq and highlights the pre-SN evolution, which lasts around 5 years, as well as the SN explosion itself. Figure A.1 provides the bolometric evolution constructed from the host-subtracted photometry presented in Fig. 3 and calibrated using the extinction and distance given in Sect. 1.

The blackbody luminosity ($L_{\rm BB}$) of the progenitor is well fitted by an accelerating (i.e. exponential) rise, followed by a fast rise after the progenitor has likely exploded. The blackbody radius ($R_{\rm BB}$) of the progenitor is seen to increase linearly at approximately 200 km s^{-1}, peaking at 1.75×10^{14} cm, after which a sharp increase is observed. This radius (~2400 $R_\odot$) is unlikely to represent the photosphere of the progenitor star, but perhaps signifies an extended or inflated envelope due to the final stages of a binary merger event (Ivanova et al. 2013; Irani et al. 2023) or a confined CSM, as this value is consistent with the shock breakout radius reported for SN 2023ixf (Zimmerman et al. 2023). Assuming this second increase is a result of core collapse, we extrapolated backwards to $R_{\rm BB} \approx 0$ cm and find an explosion time ($t_{\rm exp}$) of −13.9 days. Due to our sparse photometry around the explosion epoch, we are uncertain whether SN 2023fyq follows the

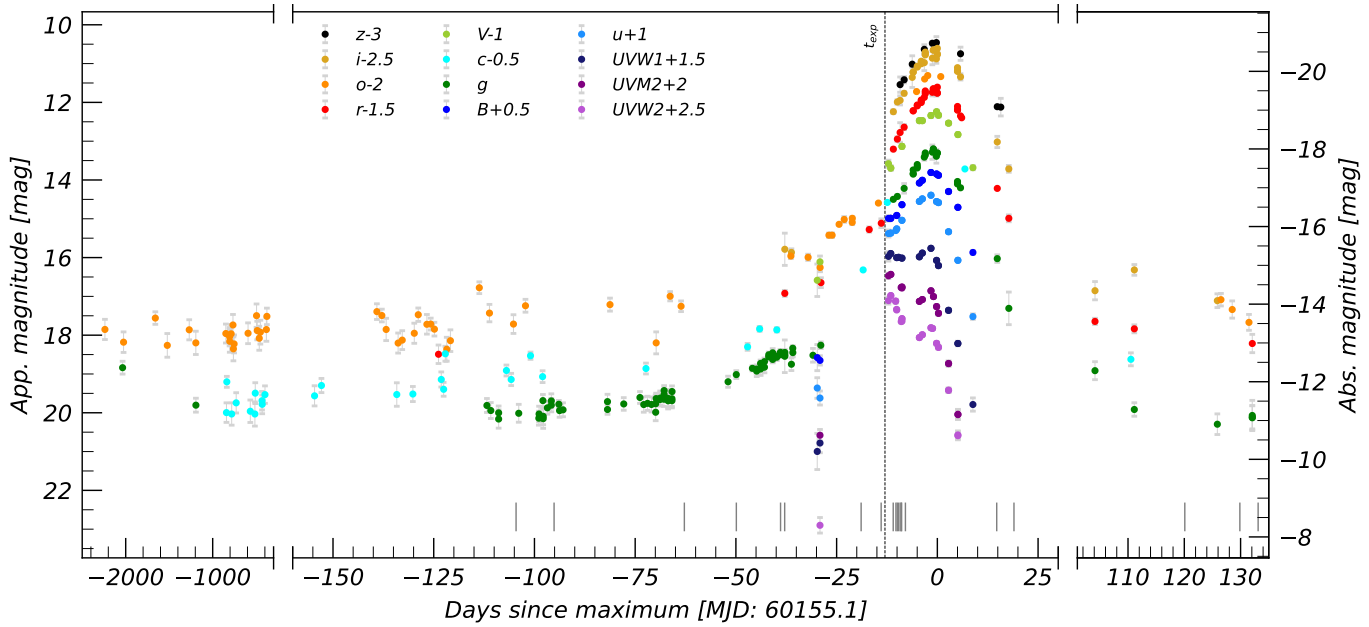

Fig. 3. Multi-band light curve of SN 2023fyq, with each band offset for clarity. Vertical grey bars denote epochs of spectral observations. Absolute magnitudes, based on a distance of 17.2 Mpc, are shown on the right *Y*-axis, uncorrected for MW or host extinction. Note the broken *X*-axis, which highlights the long-lived progenitor activity.

evolution depicted by the analytical fits in Fig. A.1 or rather a multi-component rise (e.g. SN 2021qqp and SN 2009ip; Hiramatsu et al. 2023). We adopted a rise time for SN 2023fyq of approximately 14 days, which is consistent with what is seen in other Type Ibn SNe (Hosseinzadeh et al. 2017).

From SN 2023fyq, we measure a max luminosity of 4.2×10^{43} erg s^{-1}, $L(t = t_{\rm peak}) \approx 2.2 \times 10^{41}$ erg s^{-1} and a total radiated energy of 6.0×10^{49} erg. These values are consistent with predicted activity from binary interactions (Tsuna et al. 2024) and similar to the progenitor activity in other SNe (Strotjohann et al. 2021). We measure the radiated energy of the pre-SN evolution to be $L(t < t_{\rm exp}) \approx 6.6 \times 10^{47}$ erg. Due to the lack of UV and IR coverage of the progenitor and SN 2023fyq, these values are taken as lower limits. After the SN has occurred, a dramatic increase in $L_{\rm BB}$ and $T_{\rm BB}$ is observed, with temperatures reaching ∼30 kK. This brightness increase is mainly seen in the bluer bands (see Fig. 3) and is consistent with shock breakout (e.g. SN 2008D; Chevalier & Fransson 2008; Modjaz et al. 2009).

Assuming an efficient conversion of kinetic energy to radiation, we get $M_{\rm CSM} \approx \frac{2E_{\rm rad}}{\epsilon v^2} \approx 0.05\ M_\odot$, assuming 50% energy conversion, and a velocity of 1700 km s^{-1} (taken from the observed P Cygni minimum in pre-SN spectra). This material would be very optically thick at 10^{14} cm, which is consistent with the observed thermalised spectra. For SN 2023fyq, a CSM breakout with ∼0.05 $M_\odot$ would last a few days, with a peak luminosity of a few times 10^{43} erg s^{-1}, followed by shock emergence and cooling, consistent with Fig. A.1. In this scenario (i.e. an edge-breakout or heavy CSM scenario; Khatami & Kasen 2023), we expect $M_{\rm ejecta} > M_{\rm CSM}$, and given the higher mass and lower velocity of the shocked CSM material, we expect the cooling emission to diffuse out on a longer timescale (Piro 2015). We estimate the diffusion time (taken to be $t_{\rm d} \approx \sqrt{\frac{\kappa M_{\rm CSM}}{vc}}$; Khatami & Kasen 2019) to be ∼12 days, assuming material expanding at 12 000 km s^{-1} (from Fig. A.1), which is roughly consistent with the adopted explosion time. Assuming that our final $R_{\rm BB}$ measurement before the adopted $t_{\rm exp}$ indicates the radius of this CSM material, we find $\log(R/R_\odot) \approx 3.4$, which overall agrees with the models from Khatami & Kasen (2023).

We measure the progenitor to have $\log(T_{\rm eff}/K) \approx 4.1 \pm 0.1$ and $\log(L/L_\odot) \approx 7.6 \pm 0.4$ from host-subtracted photometry. These values are likely super-Eddington and are reminiscent of the giant eruption of Eta Carina, which, possibly through multi-star interactions, ejected ∼10 $M_\odot$ of material but did not unbind the star (Smith 2011; Prieto et al. 2014). This suggests a multi-star scenario, although without detailed late-time stellar evolutionary modelling the mechanism powering the pre-SN evolution is unclear.

3.2. Spectroscopic evolution

Observations of CCSN progenitors are rare, with the only previous examples, to our knowledge, being SN 2009ip (Smith et al. 2010; Foley et al. 2011; Pastorello et al. 2013) and SN 2015bh (Elias-Rosa et al. 2016; Thöne et al. 2017). In agreement with stellar evolutionary theory, the progenitor of the Type Ibn SN 2023fyq displays features expected for He-rich stars (Crowther 2007; Yoon et al. 2010). Figure B.1 shows the evolution of He I λ5876 during the pre- and post-SN epochs, as well as the post-peak appearance. Similar to the Hα profile seen for SN 2009ip[5] in 2009 (Pastorello et al. 2013), SN 2023fyq shows a complex P Cygni-like profile for He I λ5876 (and for other He I lines) with an absorption centred at −1700 km s^{-1} and extending out to −2500 km s^{-1}. Perhaps similarly to the Hα in the late-time spectra of SN 2009ip (Fraser et al. 2015), the He I in SN 2023fyq shows a redshifted emission peak centred at +1400 km s^{-1}, which is present during the slow pre-SN rise as well as after the explosion. The velocities of these profiles do not evolve significantly during the pre-SN stage, although this may be a result of a poor S/N.

[5] Although SN 2009ip is a H-rich Type IIn SN and SN 2023fyq a H-poor Type Ibn SN, we make qualitative comparisons between the appearance of their progenitor star and their environments.

A spectrum of the explosion site from VLT/MUSE taken ∼2 years prior to SN 2023fyq is given in Fig. 2. We investigated if any potential flux from the progenitor activity is present in this spectrum by comparing it to a similar spectrum extracted at 2.4″. We note a tentative broad excess at the position of He I $\lambda\lambda$ 6678,7065 that is possibly due to progenitor emission.

Due to the sodium laser guide star, the wavelength range covering He I λ5876 is masked, preventing any investigation of a potential host contamination of He I λ5876 for SN 2023fyq. We suspect this redshifted component is originating from He I λ5876 as it is seen in several He I lines in the pre-SN spectra as well as in a similar emission component at similar velocities seen in the post-SN spectra. This would mean that the asymmetric material responsible for this emission was not destroyed in the SN explosion. SN ejecta interacting with asymmetric CSM has been used to explain irregular emission line profiles (e.g. Leloudas et al. 2015; Andrews & Smith 2018; Pursiainen et al. 2022; Hosseinzadeh et al. 2022; Smith et al. 2023) and bumpy light curves (Nyholm et al. 2017; Woosley 2018; Wang et al. 2022), and SN 2023fyq provides the first clear spectroscopic evidence of an asymmetric structure prior to core collapse.

A broad component is observed for the He I λ5876 profile in the −37 d and −17 d spectra, with wings extending to ±13 000 km s^{-1} and a full width half maximum around 14 000 km s^{-1}. Such velocities are normally associated with SN ejecta, although they have also been observed in non-terminal eruptions (Pastorello et al. 2013; Smith et al. 2018). To investigate if this broad component evolves, we measured the flux in a small wavelength bin around 5800 Å in the continuum-subtracted flux-calibrated spectra. An order of magnitude increase in flux from −103 to −10 days is observed. This confirms that the broad component rapidly evolved in strength prior to the explosion of SN 2023fyq rather than simply not being detectable in earlier spectra due to low signal-to-noise.

While these features may represent fast moving material, an alternative explanation could be electron scattering. Some mechanism(s) cause the progenitor to be surrounded by a dense CSM (such as acoustic waves or a merger; Smith 2011; Yoon et al. 2017; Fuller & Ro 2018; Chevalier 2012; Fransson et al. 2022; Tsuna et al. 2024) and may lead to shock dissipation and emission of radiation in the optically thick CSM. We modelled the −17 d spectrum using the electron scattering model from Brennan et al. (2023), assuming $V_{\rm shock}$ = 1700 km s^{-1}, $\rho \propto r^{-2}$, $\tau_{\rm e} \approx 18$, $T_{\rm e} = 2 \times 10^4$ K, and $R_2 = 1.75 \times 10^{14}$ cm. As shown in Fig. B.1, the model reproduces the wings of He I λ5876 well, suggesting that, under certain conditions, material moving at $>10^4$ km s^{-1} is not required to produce the broad features seen during the pre-SN phase. Assuming a random walk, the diffusion time is $t_d = \frac{R^2}{\lambda_{\rm mfp} c} \approx 4$ days. Our models do not produce the P Cygni-like profile or offset emission and are poorly fit in the red wing, highlighting the complex geometry likely responsible for these features.

The post-SN He I λ5876 appears double peaked with profiles that have a similar shape as those seen in the Ca II $\lambda\lambda$8498, 8542, 8662 near-IR triplet. Double-peaked emission lines have been observed in Type Ibn SNe (e.g. SN 2018bcc Karamehmetoglu et al. 2021) as well as Type IIn SNe (Brennan et al. 2022a; Hiramatsu et al. 2023) and are attributed to asymmetric SN ejecta or CSM, or both (Andrews et al. 2019; Pursiainen et al. 2022).

A longstanding question for SN 2009ip-like transients is whether the transient is indeed a SN or rather a 'SN impostor' (Van Dyk et al. 2000; Mauerhan et al. 2013; Fraser et al. 2013; Brennan et al. 2022b; Smith et al. 2022). As shown in Figs. 2 and B.1, SN 2023fyq shows broad emission from [O I] $\lambda\lambda$6300, 6364 at nebular phases, indicating that SN 2023fyq is a genuine CCSN (Jerkstrand et al. 2014; Kuncarayakti et al. 2015) whose progenitor underwent some form of instability shortly before core collapse. Late-time follow-up of SN 2023fyq reveals significant reddening due to possible dust formation. We note the appearance of O I and C I emission lines, which means the environment of SN 2023fyq is conducive for amorphous and graphite dust grains.

Events like SN 2023fyq and SN 2009ip suggest that certain massive stars experience eruptive activity preceding core collapse. However, several nearby transients lack notable eruptive activity (Jacobson-Galán et al. 2022; Ransome et al. 2023; Dong et al. 2023), implying that diverse mechanisms are responsible for pre-SN emissions in the final stages before core collapse.

4. Conclusion

In this Letter we have presented an unprecedented dataset of progenitor activity of a Type Ibn SN almost 150 days before core collapse occurs. Pre-SN spectra reveal a complex evolving He I profile. These observations of SN 2023fyq and the final moments of the progenitor demonstrate that the progenitors of CCSNe can undergo some extreme instabilities shortly before their final demise.

Progenitor analysis is typically carried out after the star has been destroyed, via searches through archival images and by measuring the photometric properties of the assumed progenitor. Although this area of transient astronomy is in its infancy, the repercussions of detecting precursor activity are immense: it indicates that the progenitor is not in a equilibrium state and may not be represented well by standard stellar evolutionary models. SN 2023fyq and similar transients underscore the fact that the pre-SN appearance of the progenitor is non-trivial and, without careful consideration, could lead to misleading results in SN progenitor studies.

Acknowledgements. We thank the anonymous referee for their comments on host extinction and CSM mass, which have improved the paper. SJB would like to thank M. Fraser and A. Guinness for their insights into late time stellar evolution and precursor events. SJB and RL acknowledges their support by the European Research Council (ERC) under the European Union's Horizon Europe research and innovation programme (grant agreement No. 10104229 – TransPIre). S. Schulze is partially supported by LBNL Subcontract NO. 7707915 and by the G.R.E.A.T. research environment, funded by Vetenskapsrådet, the Swedish Research Council, project number 2016-06012. Based on observations obtained with the Samuel Oschin Telescope 48-inch and the 60-inch Telescope at the Palomar Observatory as part of the Zwicky Transient Facility project. ZTF is supported by the National Science Foundation under Grant No. AST-2034437 and a collaboration including Caltech, IPAC, the Weizmann Institute of Science, the Oskar Klein Center at Stockholm University, the University of Maryland, Deutsches Elektronen-Synchrotron and Humboldt University, the TANGO Consortium of Taiwan, the University of Wisconsin at Milwaukee, Trinity College Dublin, Lawrence Livermore National Laboratories, IN2P3, University of Warwick, Ruhr University Bochum and Northwestern University. Operations are conducted by COO, IPAC, and UW. SED Machine is based upon work supported by the National Science Foundation under Grant No. 1106171. This work was supported by the GROWTH project funded by the National Science Foundation under Grant No 1545949. The Oskar Klein Centre is funded by the Swedish Research Council. The data presented here were obtained in part with ALFOSC, which is provided by the Instituto de Astrofisica de Andalucia (IAA) under a joint agreement with the University of Copenhagen and NOT. The ZTF forced-photometry service was funded under the Heising-Simons Foundation grant #12540303 (PI: Graham). The Gordon and Betty Moore Foundation, through both the Data-Driven Investigator Program and a dedicated grant, provided critical funding for SkyPortal. The Liverpool Telescope is operated on the island of La Palma by Liverpool John Moores University in the Spanish Observatorio del Roque de los Muchachos of the Instituto de Astrofisica de Canarias with financial

support from the UK Science and Technology Facilities Council. Based on observations obtained at the international Gemini Observatory, a program of NSF's NOIRLab, which is managed by the Association of Universities for Research in Astronomy (AURA) under a cooperative agreement with the National Science Foundation on behalf of the Gemini Observatory partnership: the National Science Foundation (United States), National Research Council (Canada), Agencia Nacional de Investigación y Desarrollo (Chile), Ministerio de Ciencia, Tecnología e Innovación (Argentina), Ministério da Ciência, Tecnologia, Inovações e Comunicações (Brazil), and Korea Astronomy and Space Science Institute (Republic of Korea). The Gemini observations were obtained through program GN-2023A-Q-122 and processed using DRAGONS (Data Reduction for Astronomy from Gemini Observatory North and South). This work was enabled by observations made from the Gemini North telescope, located within the Maunakea Science Reserve and adjacent to the summit of Maunakea. We are grateful for the privilege of observing the Universe from a place that is unique in both its astronomical quality and its cultural significance.

References

Andrews, J. E., & Smith, N. 2018, MNRAS, 477, 74
Andrews, J. E., Sand, D. J., Valenti, S., et al. 2019, ApJ, 885, 43
Bacon, R., Piqueras, L., Conseil, S., Richard, J., & Shepherd, M. 2016, Astrophysics Source Code Library [record ascl:1611.003]
Bellm, E. 2014, in The Third Hot-wiring the Transient Universe Workshop, eds. P. R. Wozniak, M. J. Graham, A. A. Mahabal, & R. Seaman, 27
Bellm, E. C., Kulkarni, S. R., Graham, M. J., et al. 2019, PASP, 131, 018002
Blagorodnova, N., Neill, J. D., Walters, R., et al. 2018, PASP, 130, 035003
Böhringer, H., Neumann, D. M., Schindler, S., & Huchra, J. P. 1997, ApJ, 485, 439
Brennan, S. J., & Fraser, M. 2022, A&A, 667, A62
Brennan, S. J., Fraser, M., Johansson, J., et al. 2022a, MNRAS, 513, 5642
Brennan, S. J., Fraser, M., Johansson, J., et al. 2022b, MNRAS, 513, 5666
Brennan, S. J., Schulze, S., Lunnan, R., et al. 2023, A&A, submitted [arXiv:2312.13280]
Cardelli, J. A., Clayton, G. C., & Mathis, J. S. 1989, ApJ, 345, 245
Chambers, K. C., Magnier, E. A., Metcalfe, N., et al. 2016, arXiv e-prints [arXiv:1612.05560]
Chevalier, R. A. 2012, ApJ, 752, L2
Chevalier, R. A., & Fransson, C. 2008, ApJ, 683, L135
Coughlin, M. W., Bloom, J. S., Nir, G., et al. 2023, ApJS, 267, 31
Crowther, P. A. 2007, ARA&A, 45, 177
Crowther, P. 2012, Astron. Geophys., 53, 4.30
Damas-Segovia, A., Beck, R., Vollmer, B., et al. 2016, ApJ, 824, 30
De, K. 2023, Transient Name Server Discovery Report, 2023–825, 1
De, K., Kasliwal, M. M., Tzanidakis, A., et al. 2020, ApJ, 905, 58
Dekany, R., Smith, R. M., Riddle, R., et al. 2020, PASP, 132, 038001
Dessart, L., Livne, E., & Waldman, R. 2010, MNRAS, 405, 2113
Dong, Y., Sand, D. J., Valenti, S., et al. 2023, ApJ, 957, 28
Ekholm, T., Lanoix, P., Teerikorpi, P., Fouqué, P., & Paturel, G. 2000, A&A, 355, 835
Elias-Rosa, N., Pastorello, A., Benetti, S., et al. 2016, MNRAS, 463, 3894
Foley, R. J., Smith, N., Ganeshalingam, M., et al. 2007, ApJ, 657, L105
Foley, R. J., Berger, E., Fox, O., et al. 2011, ApJ, 732, 32
Fransson, C., Sollerman, J., Strotjohann, N. L., et al. 2022, A&A, 666, A79
Fraser, M., Magee, M., Kotak, R., et al. 2013, ApJ, 779, L8
Fraser, M., Kotak, R., Pastorello, A., et al. 2015, MNRAS, 453, 3886
Freudling, W., Romaniello, M., Bramich, D. M., et al. 2013, A&A, 559, A96
Fuller, J., & Ro, S. 2018, MNRAS, 476, 1853
Gehrels, N., Chincarini, G., Giommi, P., et al. 2004, ApJ, 611, 1005
Graham, M. J., Kulkarni, S. R., Bellm, E. C., et al. 2019, PASP, 131, 078001
Heger, A., Fryer, C. L., Woosley, S. E., Langer, N., & Hartmann, D. H. 2003, ApJ, 591, 288
Hiramatsu, D., Matsumoto, T., Berger, E., et al. 2023, ApJ, submitted [arXiv:2305.11168]
Hook, I. M., Jørgensen, I., Allington-Smith, J. R., et al. 2004, PASP, 116, 425
Hosseinzadeh, G., Arcavi, I., Valenti, S., et al. 2017, ApJ, 836, 158
Hosseinzadeh, G., Kilpatrick, C. D., Dong, Y., et al. 2022, ApJ, 935, 31
Humphreys, R. M., & Davidson, K. 1994, PASP, 106, 1025
Irani, I., Morag, J., Gal-Yam, A., et al. 2023, ApJ, submitted [arXiv:2310.16885]
Ivanova, N., Justham, S., Chen, X., et al. 2013, A&ARv, 21, 59
Jacobson-Galán, W. V., Dessart, L., Jones, D. O., et al. 2022, ApJ, 924, 15
Janka, H.-T. 2012, Ann. Rev. Nucl. Part. Sci., 62, 407
Jerkstrand, A., Smartt, S. J., Fraser, M., et al. 2014, MNRAS, 439, 3694
Karamehmetoglu, E., Fransson, C., Sollerman, J., et al. 2021, A&A, 649, A163
Kashi, A., Soker, N., & Moskovitz, N. 2013, MNRAS, 436, 2484
Khatami, D., & Kasen, D. 2023, ApJ, submitted [arXiv:2304.03360]
Khatami, D. K., & Kasen, D. N. 2019, ApJ, 878, 56
Kilpatrick, C. D., Foley, R. J., Drout, M. R., et al. 2018, MNRAS, 473, 4805
Kim, Y. L., Rigault, M., Neill, J. D., et al. 2022, PASP, 134, 024505
Kuncarayakti, H., Maeda, K., Bersten, M. C., et al. 2015, A&A, 579, A95
Labrie, K., Anderson, K., Cárdenes, R., Simpson, C., & Turner, J. E. H. 2019, ASP Conf. Ser., 523, 321
Leloudas, G., Hsiao, E. Y., Johansson, J., et al. 2015, A&A, 574, A61
Leung, S.-C., Wu, S., & Fuller, J. 2021, ApJ, 923, 41
Lianou, S., Barmby, P., Mosenkov, A. A., Lehnert, M., & Karczewski, O. 2019, A&A, 631, A38
Mandigo-Stoba, M. S., Fremling, C., & Kasliwal, M. 2022, J. Open Source Softw., 7, 3612
Margutti, R., Milisavljevic, D., Soderberg, A. M., et al. 2014, ApJ, 780, 21
Masci, F. J., Laher, R. R., Rusholme, B., et al. 2019, PASP, 131, 018003
Matsumoto, T., & Metzger, B. D. 2022, ApJ, 936, 114
Mattila, S., Meikle, W. P. S., Lundqvist, P., et al. 2008, MNRAS, 389, 141
Mauerhan, J. C., Smith, N., Filippenko, A. V., et al. 2013, MNRAS, 430, 1801
Modjaz, M., Li, W., Butler, N., et al. 2009, ApJ, 702, 226
Müller, B., SViallet, M., Heger, A., & Janka, H. T. 2016, ApJ, 833, 124
Nyholm, A., Sollerman, J., Taddia, F., et al. 2017, A&A, 605, A6
Ofek, E. O., Sullivan, M., Cenko, S. B., et al. 2013, Nature, 494, 65
Ofek, E. O., Sullivan, M., Shaviv, N. J., et al. 2014, ApJ, 789, 104
Oke, J. B., Cohen, J. G., Carr, M., et al. 1995, PASP, 107, 375
Osterbrock, D. E. 1989, Astrophysics of Gaseous Nebulae and Active Galactic Nuclei (University Science Books)
Pastorello, A., Smartt, S. J., Mattila, S., et al. 2007, Nature, 447, 829
Pastorello, A., Cappellaro, E., Inserra, C., et al. 2013, ApJ, 767, 1
Perley, D. A. 2019, PASP, 131, 084503
Piro, A. L. 2015, ApJ, 808, L51
Prieto, J. L., Rest, A., Bianco, F. B., et al. 2014, ApJ, 787, L8
Prochaska, J. X., Hennawi, J., Cooke, R., et al. 2020a, https://doi.org/10.5281/zenodo.3743493
Prochaska, J. X., Hennawi, J. F., Westfall, K. B., et al. 2020b, J. Open Source Softw., 5, 2308
Pursiainen, M., Leloudas, G., Paraskeva, E., et al. 2022, A&A, 666, A30
Quataert, E., & Shiode, J. 2012, MNRAS, 423, L92
Ransome, C. L., Villar, V. A., Tartaglia, A., et al. 2023, arXiv e-prints [arXiv:2312.04426]
Rigault, M., Neill, J. D., Blagorodnova, N., et al. 2019, A&A, 627, A115
Roming, P. W. A., Kennedy, T. E., Mason, K. O., et al. 2005, Space. Sci. Rev., 120, 95
Schlafly, E. F., & Finkbeiner, D. P. 2011, ApJ, 737, 103
Shingles, L., Smith, K. W., Young, D. R., et al. 2021, Transient Name Server AstroNote, 7, 1
Siebert, M. R., Foley, R. J., Jones, D. O., et al. 2019, MNRAS, 486, 5785
Smith, N. 2011, MNRAS, 415, 2020
Smith, N., & Arnett, W. D. 2014, ApJ, 785, 82
Smith, N., Miller, A., Li, W., et al. 2010, AJ, 139, 1451
Smith, N., Rest, A., Andrews, J. E., et al. 2018, MNRAS, 480, 1457
Smith, K. W., Smartt, S. J., Young, D. R., et al. 2020, PASP, 132, 085002
Smith, N., Andrews, J. E., Filippenko, A. V., et al. 2022, MNRAS, 515, 71
Smith, N., Pearson, J., Sand, D. J., et al. 2023, ApJ, 956, 46
Strotjohann, N. L., Ofek, E. O., Gal-Yam, A., et al. 2021, ApJ, 907, 99
Thöne, C. C., de Ugarte Postigo, A., Leloudas, G., et al. 2017, A&A, 599, A129
Tonry, J. L., Denneau, L., Heinze, A. N., et al. 2018, PASP, 130, 064505
Tsang, B. T. H., Kasen, D., & Bildsten, L. 2022, ApJ, 936, 28
Tsuna, D., Matsumoto, T., Wu, S. C., & Fuller, J. 2024, ApJ, submitted [arXiv:2401.02389]
Valerin, G., Benetti, S., Elias-Rosa, N., et al. 2023, Transient Name Server Classification Report, 2023–1777, 1
van der Walt, S., Crellin-Quick, A., & Bloom, J. 2019, The J. Open Source Softw., 4, 1247
Van Dyk, S. D., Peng, C. Y., King, J. Y., et al. 2000, PASP, 112, 1532
Wang, L.-J., Liu, L.-D., Lin, W.-L., et al. 2022, ApJ, 933, 102
Weilbacher, P. M., Palsa, R., Streicher, O., et al. 2020, A&A, 641, A28
Woosley, S. E. 2018, ApJ, 863, 105
Woosley, S. E., & Weaver, T. A. 1995, ApJS, 101, 181
Woosley, S. E., Blinnikov, S., & Heger, A. 2007, Nature, 450, 390
Wu, S., & Fuller, J. 2022, Am. Astron. Soc. Meeting Abstracts, 54, 32707
Yaron, O., & Gal-Yam, A. 2012, PASP, 124, 668
Yoon, S. C., Woosley, S. E., & Langer, N. 2010, ApJ, 725, 940
Yoon, S.-C., Dessart, L., & Clocchiatti, A. 2017, ApJ, 840, 10
Zapartas, E., de Mink, S. E., Justham, S., et al. 2021, A&A, 645, A6
Zimmerman, E. A., Irani, I., Chen, P., et al. 2023, Nature, 627, 759

Appendix A: Bolometric Evolution of SN 2023fyq and it's progenitor

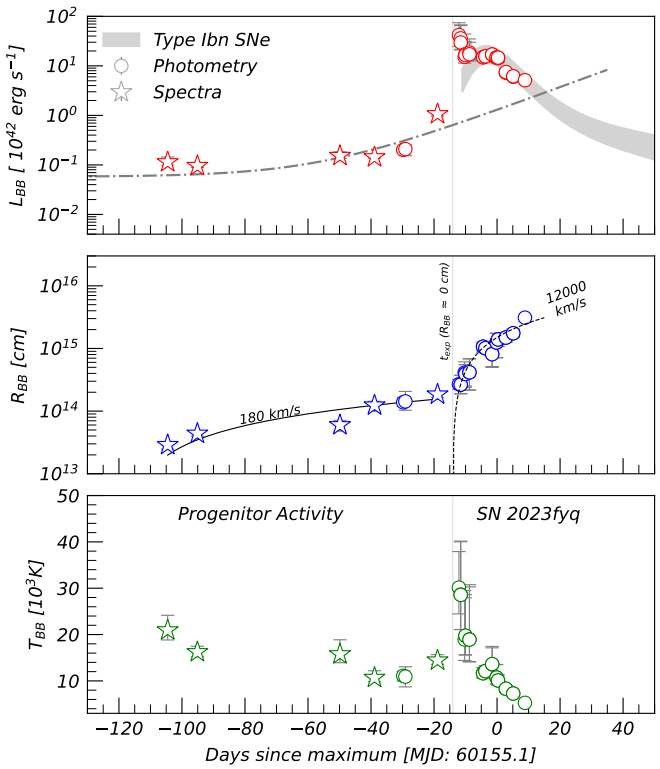

Fig. A.1. Blackbody luminosity of SN 2023fyq and its progenitor. Star markers indicate blackbody fits to the synthetic photometry from spectra presented in Fig. 2. Circle markers are blackbody fits to epochs of photometry that contain at least *u*-band observations. The blackbody radius and temperature are provided in the middle and lower panels, respectively.

Appendix B: Evolution of the He I λ5876 profile

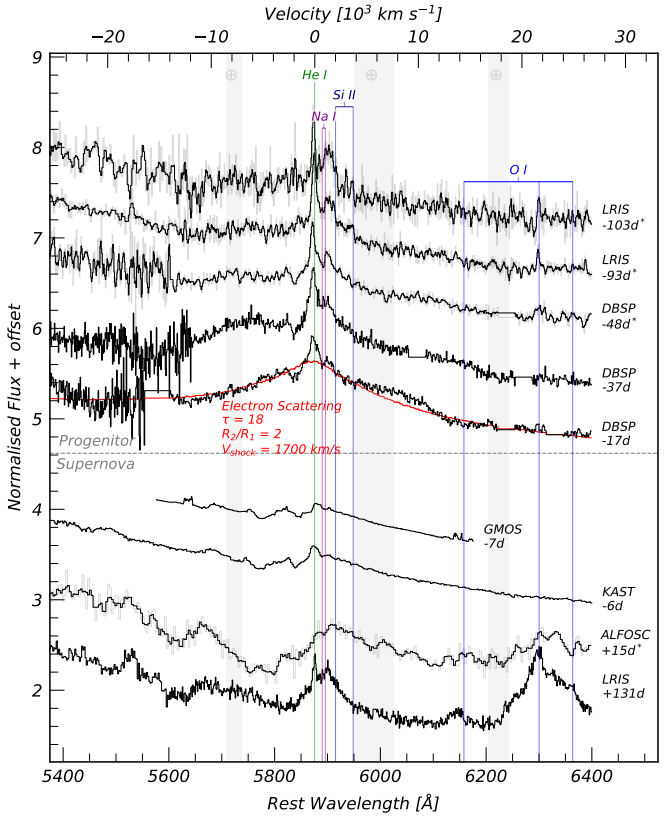

Fig. B.1. Evolution of the He I λ5876 emission profile. Pre-SN spectra show complex P Cygni-like profiles. Soon after the SN occurs, an additional absorption component is seen in the −6d Lick/Kast spectrum at around −5000 km s^{-1}. At late times, the P Cygni absorption is no longer observed, but rather a double-peaked emission profile consisting of host emission and redshifted He I emission at similar velocities as seen in the −93d Keck/LRIS spectrum. Spectra marked with an asterisk have been re-binned for clarity, with the raw spectrum given in grey. We manually masked out telluric lines and artefacts from the sky subtractions.